Stretchable and compressible thin films of stiff materials on compliant wavy substrates

J. Xiao,[1] A. Carlson,[2] Z. J. Liu,[3] Y. Huang,[1,4,a)] H. Jiang,[5] and J. A. Rogers[2,6,b)]

[1]*Department of Mechanical Engineering, Northwestern University, Evanston, Illinois 60208, USA*
[2]*Department of Materials Science and Engineering, University of Illinois, Urbana, Illinois 61801, USA*
[3]*Institute of High Performance Computing, Singapore 117528, Singapore*
[4]*Department of Civil and Environmental Engineering, Northwestern University, Evanston, Illinois 60208, USA*
[5]*Department of Mechanical and Aerospace Engineering, Arizona State University, Tempe, Arizona 85287, USA*
[6]*Beckman Institute and Seitz Materials Research Laboratory, University of Illinois, Urbana, Illinois 61801, USA*

This letter presents experimental, numerical, and analytical studies of Au thin films on elastomeric substrates of poly(dimethylsiloxane) that are designed with sinusoidal, "wavy" features of surface relief. Such systems can be useful as stretchable conductors in electronic or sensory devices. The maximum film strain is obtained in terms of film and substrate elastic moduli, film thickness, amplitude and wavelength of the wavy profile, and the applied strain. These analytical solutions agree well with both finite element analysis and experimentally measured changes in the sinusoidal profile under small, uniaxial strains. A simple expression for the system stretchability and compressibility is established. © *2008 American Institute of Physics.* [DOI: 10.1063/1.2955829]

Stretchable electronics have the potential to be important components of many emerging technologies, including paperlike displays,[1,2] electronic eyes,[3] bending actuators,[4] synthetic sensitive skins,[5,6] and structural health monitoring devices.[7] Previous studies have exploited the buckling of stiff nanomembranes on compliant substrates to attain multidimensional stretchability in high-performance circuits.[8–11] The mechanism and mechanics of such systems have been investigated extensively.[12–21] Although these systems have many attractive features, one disadvantage is that compressive strains in the buckled films, established in the fabrication procedures, yield stretchability at the expense of reduced compressibility. In this letter, we propose an alternative in which the stiff thin film is conformally integrated with a compliant substrate with prefabricated wavy structures of relief on its surface, thereby avoiding any initial film strain and thus achieving both high stretchability and compressibility.

Contoured compliant substrates were fabricated in a process involving a series of molding and imprinting steps from a rigid silicon template. Initially, plasma-enhanced chemical vapor deposition formed a thin (200 nm) silicon nitride layer on a Si (100) wafer (SQI, Inc.); conventional photolithography and plasma etching formed patterns of alternating lines and spaces in this nitride layer. After ashing the photoresist, anisotropic etching of the Si (100) in a 90 °C isopropyl alcohol buffered 25% KOH solution for 35 min produced the sawtooth structure in Fig. 1(a). Removing the nitride mask with concentrated (49%) HF and then spin casting a thin layer of photoresist (MicroChem S1805) at 3500 rpm for 90 s converted the sawtooth relief into an approximately sinusoidal shape.

This silicon/photoresist surface profile was replicated in a thin (300 μm) layer of elastomeric polymer such as poly-

(dimethylsiloxane) (PDMS) on a glass substrate by two consecutive casting and curing steps. The PDMS/glass element was pressed against a layer (75 μm) of negative tone photoresist (SU-8 50; MicroChem Corp.) on a thin (100 μm) plastic substrate (polyethylene terephthalate, PET), which was cured by flood exposing the system to ultraviolet light (λ=365 nm) for 30–40 s from both the top and bottom followed by a 5 min bake at 65 °C. Careful removal of the PDMS/glass produced a molded SU-8 substrate with the inverted sawtooth profile of the silicon wafer. Spin casting a layer of SU-8 2 (MicroChem Corp.) diluted to $\frac{1}{2}$ volume fraction with SU-8 thinner smoothed the relief valleys in the molded SU-8. Electron-beam deposition (Temescal
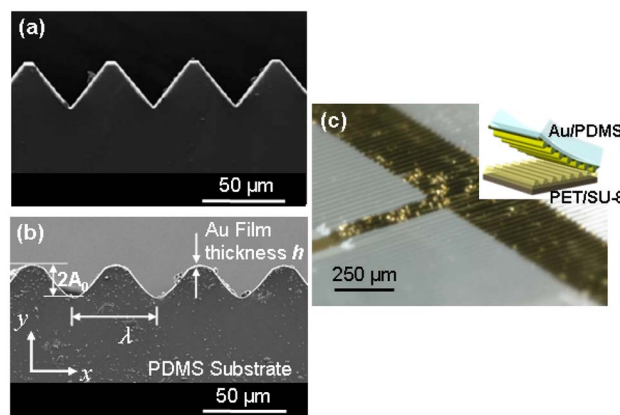

FIG. 1. (Color online) Profile of the wavy compliant substrate and stiff thin film system. Anisotropic etching of silicon produced a sawtooth pattern (a), which formed the underlying sinusoidal structure for the wavy profile. After a sequential process of smoothing, molding, and metallization, a final PDMS substrate with a thin (300 nm) gold film was obtained (b). Here $2A_0$ is the peak to valley initial amplitude, λ the wavelength, and h the thickness of the stiff thin film. (c) shows an optical image of an isolated wavy gold film created in this manner. The inset shows delamination of the contoured Au/PDMS substrate from the PET/SU-8 mold.

a)Electronic mail: y-huang@northwestern.edu.
b)Electronic mail: jrogers@uiuc.edu.

BJD1800) of Au through a shadow mask produced patterned films (300 nm thick), conformally coating the contoured SU-8 surface. Treating this substrate with mercaptopropylt-rimethoxysilane via vapor phase exposure prepared the sample for a final PDMS molding step. After casting and curing the PDMS prepolymer, fast removal of the stamp transferred the metal films to the PDMS, resulting in the wavy Au-coated profile seen in Fig. 1(b). Figure 1(c) is an optical image of an isolated thin film (300 nm) on a wavy substrate. The mechanics of these structures were examined through surface profilometry (Dektak 3030) at various levels of uniaxial strain applied with a tensioning stage.

To determine the maximum strain supported by the stiff thin film, we first used an energy method to calculate the change in profile amplitude under applied strain. The total system energy consists of three parts, the bending energy U_b due to thin film curvature changes, the membrane energy U_m, and substrate energy U_S.[8,17,18] Figure 1(b) shows a stiff thin film of thickness h on a compliant substrate having a wavy surface profile given by $y = A_0 \cos kx$, where A_0 is the initial amplitude, $k = 2\pi/\lambda$, and λ is the wavelength. For small initial amplitudes, $A_0 \ll \lambda$, the curvature of the film is $\kappa_0 = d^2y/dx^2 = -A_0 k^2 \cos kx$. After application of a small strain ε_a to the film/substrate system, the change in curvature is given as $\Delta\kappa = d^2w/dx^2 = (A_0 - A)k^2 \cos kx$, where A is the strained profile amplitude and $w = (A - A_0)\cos kx$ is the displacement in the y direction. The bending energy per unit length of the film can then be obtained using the plane-strain modulus of the film $\bar{E}_f = E_f/(1 - \nu_f^2)$ and the bending stiffness, $\bar{E}_f I = \bar{E}_f h^3/12$ via

$$U_b = \frac{1}{\lambda}\int_0^\lambda \frac{1}{2}\bar{E}_f I(\Delta\kappa)^2 dx = \frac{1}{48}\bar{E}_f h^3 (A_0 - A)^2 k^4. \quad (1)$$

The membrane strain, ε_m, which determines the energy in the thin film, depends on both the x and y direction displacements, u and w, respectively. For an infinitesimal segment of the film with initial length $dS = \sqrt{(dx)^2 + (dy)^2}$, after deformation the segment is elongated to $ds = \sqrt{(dx+du)^2 + (dy+dw)^2}$. The membrane strain is then $\varepsilon_m = (ds - dS)/dS$ which can be simplified to $\varepsilon_m = u' + (w')^2/2 + y'w'$ for small amplitudes $A_0 \ll \lambda$ and small strains, but finite rotation. Here $(\ )' = d(\ )/dx$. Since the elastic modulus of the PDMS substrate ($\sim$2 MPa) is several orders of magnitude smaller than that of Au film ($\sim$70 GPa), the effect of interface shear is negligible.[18] This conclusion is confirmed independently by the finite element analysis presented at the end of this letter. Force equilibrium of the film requires a constant membrane strain for film thickness $h \ll \lambda$, giving the displacement $u = \varepsilon_a x - (1/8)(A_0^2 - A^2)k\sin 2kx$, where ε_a is the applied strain in the x direction, and the condition $\int_0^\lambda u' dx = \varepsilon_a \lambda$ has been imposed to ensure the compatibility of deformation in the film and substrate. The membrane strain in the film is then obtained as $\varepsilon_m = \varepsilon_a - \frac{1}{4}(A_0^2 - A^2)k^2$, yielding a membrane energy per unit length of the film of

$$U_m = \frac{1}{\lambda}\int_0^\lambda \frac{1}{2}\bar{E}_f h\varepsilon_m^2 dx = \frac{1}{2}\bar{E}_f h\left[\varepsilon_a - \frac{1}{4}(A_0^2 - A^2)k^2\right]^2. \quad (2)$$

The substrate is modeled as a semi-infinite solid since its thickness is much larger than the wavelength λ. The wavy surface profile, $y = A_0 \cos kx$, can be transformed to a straight line in a new coordinate system (x, η), where $\eta = y$

$-A_0 \cos kx$. Strains are then obtained from the displacements u_x and u_y as $\varepsilon_{xx} = u_{x,x} + u_{x,\eta}A_0 k\sin kx$, $\varepsilon_{yy} = u_{y,\eta}$ and $2\varepsilon_{xy} = u_{x,\eta} + u_{y,x} + u_{y,\eta}A_0 k\sin kx$, where $(\ )_x$ and $(\ )_\eta$ represent the partial derivatives with respect to x and η. The substrate stress is determined via the linear elastic relation (Young's modulus E_S and Poisson's ratio ν_S) with the equilibrium equation providing two partial differential equations for u_x and u_y. Boundary conditions for the top surface, $\eta = 0$, are $u_y = (A - A_0)\cos kx$ and a vanishing shear traction, $\tau_{nt} = 0$, due to negligible interface shear. The remote boundary conditions require $\varepsilon_{xx}|_{\eta\to-\infty} = \varepsilon_a$ due to the applied strain and vanishing tractions. For small amplitude ($A_0 \ll \lambda$ or, equivalently, $A_0 k \ll 1$), the displacements can be written as

$$u_x = u_x^{(0)} + (A_0 k)u_x^{(1)} + (A_0 k)^2 u_x^{(2)} + \cdots,$$

$$u_y = u_y^{(0)} + (A_0 k)u_y^{(1)} + (A_0 k)^2 u_y^{(2)} + \cdots. \quad (3)$$

Substitution into the equilibrium equations and boundary conditions, together with the perturbation method, give the analytical solutions

$$u_x^{(0)} = \varepsilon_a x, \ u_y^{(0)} = -\frac{\nu_S}{1 - \nu_S}\varepsilon_a \eta, \quad (4)$$

$$u_x^{(1)} = \left[(1 - 2\nu_S + k\eta)\frac{A - A_0}{A_0} - (3 - 2\nu_S + k\eta)\varepsilon_a\right]\frac{e^{k\eta}\sin kx}{2k(1 - \nu_S)},$$

$$u_y^{(1)} = \left\{-2\nu_S\varepsilon_a + \left[(2 - 2\nu_S - k\eta)\frac{A - A_0}{A_0} + (2\nu_S + k\eta)\varepsilon_a\right]e^{k\eta}\right\}\frac{\cos kx}{2k(1 - \nu_S)}. \quad (5)$$

Expressions for $u_x^{(2)}$ and $u_y^{(2)}$ are not presented due to space limitations. The strain energy per unit length of the substrate can now be obtained by integrating $\sigma_{ij}\varepsilon_{ij}/2$ over the substrate. The derivative with respect to A is

$$\frac{dU_S}{dA} = \frac{1}{4}\bar{E}_S k(A - A_0) + \frac{1}{4}\bar{E}_S \varepsilon_a kA_0, \quad (6)$$

where $\bar{E}_S = E_S/(1 - \nu_S^2)$ is the plane-strain modulus.

Minimization of total energy with respect to the profile amplitude, $\partial U_{\text{tot}}/\partial A = 0$ yields the cubic equation $(A/A_0)^3 + p(A/A_0) - q = 0$ for A, where $p = 4\varepsilon_a/(kA_0)^2 + h^2/(3A_0^2) + 2\bar{E}_S/(\bar{E}_f k^3 hA_0^2) - 1$ and $q = h^2/(3A_0^2) + 2(1 - \varepsilon_a)\bar{E}_S/(\bar{E}_f k^3 hA_0^2)$. For small applied strains, this equation can be solved analytically for the amplitude

$$A = A_0\left[1 - \frac{6\varepsilon_a(\bar{E}_S + 2\bar{E}_f kh)}{6\bar{E}_S + \bar{E}_f kh(k^2 h^2 + 6k^2 A_0^2)}\right]. \quad (7)$$

As is evident from Eq. (7), the amplitude decreases linearly with the applied strain. Figure 2 compares simulated and measured amplitude changes for a 0.3 μm thick Au film ($E_f = 78$ GPa, $\nu_f = 0.42$) on a wavy PDMS substrate ($E_S = 2$ MPa, $\nu_S = 0.48$) under small uniaxial tension. The profile wavelength was held constant at $\lambda = 49$ μm for each of the three initial amplitudes $A_0 = 7.2$, 9.5, and 10.5 μm examined. The experimental measurements in Fig. 2 (denoted by
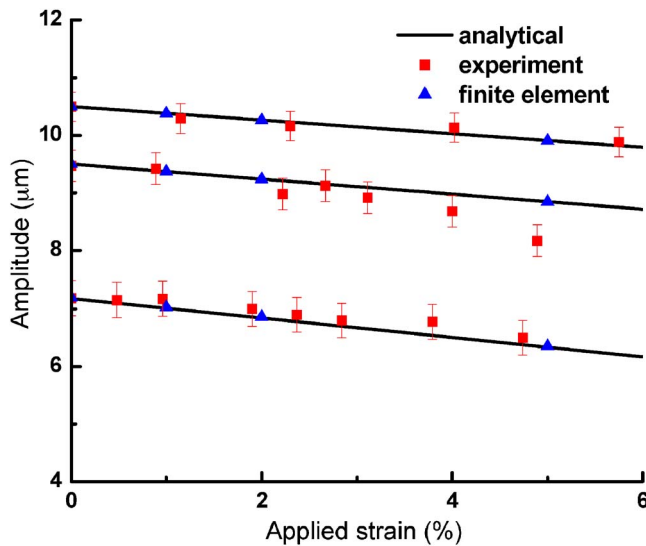
FIG. 2. (Color online) The amplitude A vs the applied strain ε_a for a 0.3 μm thick Au film (E_f=78 GPa, ν_f=0.42) on a wavy PDMS substrate (E_S=2 MPa, ν_S=0.48) with the wavelength λ=49 μm and several initial amplitudes A_0=7.2, 9.5, and 10.5 μm.

squares) and finite element method results (marked by triangles) agree remarkably well with the analytical solution of Eq. (7) without parameter fitting.

The maximum strain $\varepsilon_{\max}$ supported by the thin film can be determined by the sum of the membrane strain ε_m and the bending strain, $\varepsilon_b = \Delta\kappa h/2$ as

$$\varepsilon_{\max} = \varepsilon_a \frac{3\bar{E}_S(2 - k^2A_0^2 + k^2A_0h) + \bar{E}_f k^3 h^2(6A_0 + h)}{6\bar{E}_S + \bar{E}_f k^3 h(6A_0^2 + h^2)}. \quad (8)$$

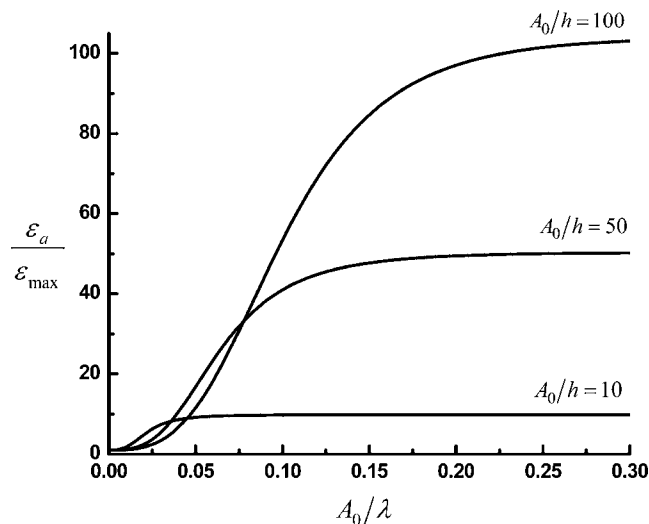Figure 3 shows the ratio of applied strain to the maximum film strain, $\varepsilon_a/\varepsilon_{\max}$, versus the ratio of initial amplitude to wavelength, A_0/λ, for A_0/h=10, 50, and 100. Each curve in Fig. 3 has a plateau at large initial amplitude (e.g., $A_0 > \lambda/5$), indicating the maximum ratio of $\varepsilon_a/\varepsilon_{\max}$. For very stiff ($\bar{E}_f \gg \bar{E}_S$) and thin film ($h \ll A_0$), the plateau is given simply by A_0/h such that the system stretchability (maximum strain before failure) is $A_0\varepsilon_c/h$, where ε_c is the failure

strain of the thin film. For Au thin film with a maximum elastic strain of ε_c=0.46% (Ref. 22) (beyond which plastic yielding occurs), the system stretchabilities are 4.6%, 23%, and 46% for A_0/h=10, 50, and 100, respectively. Therefore, for a given film thickness h, a large initial amplitude and/or small wavelength, i.e., a wavier film (and substrate), reduces film strain, making the system more stretchable.

The above analyses and results also hold for compression of the stiff thin film on a compliant wavy substrate. For example, the system compressibility is also given by $A_0\varepsilon_c/h$ for very stiff and thin films. This provides the contoured wavy film/substrate an additional range of motion not captured by other buckling systems.

FIG. 3. The ratio of applied strain to the maximum film strain, $\varepsilon_a/\varepsilon_{\max}$, vs the ratio of initial amplitude to wavelength, A_0/λ, obtained by the analytical solution for A_0/h=10, 50, and 100, where h is the film thickness.

[1] J. A. Rogers, Z. Bao, K. Baldwin, A. Dodabalapur, B. Crone, V. R. Raju, V. Kuck, H. Katz, K. Amundson, J. Ewing, and P. Drzaic, Proc. Natl. Acad. Sci. U.S.A. **98**, 4835 (2001).
[2] H. O. Jacobs, A. R. Tao, A. Schwartz, D. H. Gracias, and G. M. Whitesides, Science **296**, 323 (2002).
[3] H. C. Ko, M. P. Stoykovich, J. Song, V. Malyarchuk, W. M. Choi, C.-J. Yu, J. B. Geddes, J. Xiao, S. Wang, Y. Huang, and J. A. Rogers, "A hemispherical electronic eye camera based on compressible silicon optoelectronics," Nature (London) (unpublished).
[4] M. Watanabe, H. Shirai, and T. Hirai, J. Appl. Phys. **92**, 4631 (2002).
[5] V. Lumelsky, M. S. Shur, and S. Wagner, IEEE Sens. J. **1**, 41 (2001).
[6] T. Someya, T. Sekitani, S. Iba, Y. Kato, H. Kawaguchi, and T. Sakurai, Proc. Natl. Acad. Sci. U.S.A. **101**, 9966 (2004).
[7] A. Nathan, B. Park, A. Sazonov, S. Tao, I. Chan, P. Servati, K. Karim, T. Charania, D. Striakhilev, Q. Ma, and R. V. R. Murthy, Microelectron. J. **31**, 883 (2000).
[8] D. Y. Khang, H. Jiang, Y. Huang, and J. A. Rogers, Science **311**, 208 (2006).
[9] D.-H. Kim, J.-H. Ahn, W. M. Choi, H.-S. Kim, T.-H. Kim, J. Song, Y. Y. Huang, Z. J. Liu, C. Lu, and J. A. Rogers, Science **320**, 507 (2008).
[10] W. M. Choi, J. Song, D.-Y. Khang, H. Jiang, Y. Y. Huang, and J. A. Rogers, Nano Lett. **7**, 1655 (2007).
[11] Y. Sun, W.-M. Choi, H. Jiang, Y. Huang, and J. A. Rogers, Nat. Nanotechnol. **1**, 201 (2006).
[12] N. Bowden, S. Brittain, A. G. Evans, J. W. Hutchinson, and G. M. Whitesides, Nature (London) **393**, 146 (1998).
[13] J. Kim and H. H. Lee, J. Polym. Sci., Part B: Polym. Phys. **39**, 1122 (2001).
[14] R. Huang and Z. Suo, J. Appl. Phys. **91**, 1135 (2002).
[15] S. P. Lacour, S. Wagner, Z. Huang, and Z. Suo, Appl. Phys. Lett. **82**, 2404 (2003).
[16] J. Genzer and J. Groenewold, Soft Matter **2**, 310 (2006).
[17] X. Chen and J. W. Hutchinson, J. Appl. Mech. **71**, 597 (2004).
[18] Z. Y. Huang, W. Hong, and Z. Suo, J. Mech. Phys. Solids **53**, 2101 (2005).
[19] H. Jiang, D.-Y. Khang, J. Song, Y. Sun, Y. Huang, and J. A. Rogers, Proc. Natl. Acad. Sci. U.S.A. **104**, 15607 (2007).
[20] H. Jiang, Y. Sun, J. A. Rogers, and Y. Huang, Appl. Phys. Lett. **90**, 133119 (2007).
[21] C. T. Koh, Z. J. Liu, D.-Y. Khang, J. Song, C. Lu, Y. Huang, J. A. Rogers, and C. G. Koh, Appl. Phys. Lett. **91**, 133113 (2007).
[22] T. P. Weihs, S. Hong, J. C. Bravman, and W. D. Nix, J. Mater. Res. **3**, 931 (1988).